DOI: 10.1002/chem.200601349

Control of Channel Shapes in a Microporous Manganese(II)–Borophosphate Framework by Variation of Size and Shape of Organic Template Cations

Ya-Xi Huang, Oliver Hochrein, Dirk Zahn, Yurii Prots, Horst Borrmann, and Rüdiger Kniep*[a]

Abstract: The templated microporous compounds $[H_2(Templ.)][Mn^{II}\{B_2P_3O_{12}(OH)\}]$, [templates: 1,3-diaminopropane, $C_3H_{10}N_2$ (DAP); piperazine, $C_4H_{10}N_2$ (PIP); 1,4-diazacyclo-[2.2.2]octane, $C_6H_{12}N_2$ (DABCO)] were prepared under mild hydrothermal conditions. The crystal structures (H_2DAP-Mn: $Pmc2_1$ (no. 26), $a=1259.43(5)$, $b=949.86(5)$, $c=1135.92(5)$ pm, $Z=4$; H_2PIP-Mn: $Ima2$ (no. 46), $a=1257.9(1)$, $b=948.69(8)$, $c=1158.19(8)$ pm, $Z=4$; H_2DABCO-H_2PIP-Mn: $Ima2$ (no. 46), $a=1262.90(7)$, $b=961.05(5)$, $c=1151.42(7)$ pm, $Z=4$) are characterized by identical framework connectivities $[Mn^{II}\{B_2P_3O_{12}(OH)\}]^{2-}$, but vary in shapes (diameters) of the structural channels depending on the shapes of the templating molecule ions. The situation clearly reflects the directing effect of true templates during endotemplating reactions. The experimental results (preparation, chemical analyses, and X-ray refinements) are supported by detailed ab initio calculations (structure optimizations).

Keywords: ab initio calculations · borophosphate · manganese · microporous materials · template synthesis

Introduction

Ferdi Schüth commented in his recent review on templating that "this term creates the impression of a 1:1 correspondence between shape of the molecule used as template and shape of the void remaining after template removal".[1] Here, we report on templated microporous compounds with general composition $[H_2(Templ.)][Mn^{II}\{B_2P_3O_{12}(OH)\}]$ revealing identical framework connectivities $[Mn^{II}\{B_2P_3O_{12}(OH)\}]^{2-}$, but differing in shape and size of the structural channels depending on the shape and size of the organic molecule used as the templating agent. It becomes clear already from the general formula of the compounds under consideration that calcination in order to remove the organic component is not possible because of collapsing the framework. In this way, the second part of the definition given above (removal of the template) does not hold for the Mn^{II}–borophosphates. On the other hand, Schüth additionally states[1] that the most convincing criterion for an additive operating as a "true template" is given by a "framework being formed around the organic molecule which determines the shape and size of the later voids in the structure".

By focusing our reflections on "true templates" with a directing effect on a microporous framework with a given (constant) connectivity, a shape–control interaction is then restricted to a significant intrinsic flexibility of the framework structure. There is one prominent example originating from materials (tetrahedral frameworks) with RHO topology in which the alteration of endotemplating alkali ions and the degree of hydrate water causes framework distortions connected with twisting of eight-membered alumosilicate/alumogermanate rings.[2] It is evident that definite proof for true endotemplating reactions taking place during the synthesis of a templated inorganic material are only difficult to offer, unless the reaction mechanisms are elucidated in detail by suitable in-situ methods.[1] Even this procedure is a hard one in complex systems. On the other hand, also the lucky chance is very likely, to find a chemical system from which different templated compounds with the same inorganic framework connectivity can be prepared just by variation of the organic molecules. In this context we were successful in preparing a number of templated Mn^{II}–borophosphates by mild hydrothermal treatment of aqueous mixtures of $MnCl_2$, H_3BO_3, H_3PO_4 with either 1,3-diaminopropane ($C_3H_{10}N_2$, DAP), piperazine ($C_4H_{10}N_2$, PIP), or even 1,4-

[a] Dr. Y.-X. Huang, Dr. O. Hochrein, Dr. D. Zahn, Dr. Y. Prots, Dr. H. Borrmann, Prof. Dr. R. Kniep
Max-Planck-Institut für Chemische Physik fester Stoffe
Nöthnitzer Str. 40, 01187 Dresden (Germany)
Fax: (+49) 351-4646-3002
E-mail: kniep@cpfs.mpg.de

 © 2007 Wiley-VCH Verlag GmbH & Co. KGaA, Weinheim

diazacyclo[2.2.2]octane ($C_6H_{12}N_2$, DABCO) used as an endotemplating agent, after structure optimization calculations had indicated this general chance. The compounds under consideration will be denoted as H_2DAP-Mn, H_2PIP-Mn, "H_2DABCO-Mn", and H_2DABCO-H_2PIP-Mn, respectively.

Results and Discussion

The crystal structures of H_2DAP-Mn and H_2PIP-Mn (see Experimental Section for details of data collection and Table 1) contain undulated chains of formula $^1_\infty\{[B_2P_3O_{12}(OH)]^{4-}\}$, which are built up from BO_4, PO_4 and $(HO)PO_3$ tetrahedra (Figure 1). The central backbone of the chains is characterised by a sequence of two BO_4 tetrahedra followed by one PO_4 tetrahedron. The terminal corners of the adjacent (condensed) BO_4 tetrahedra are loop-branched by one additional PO_4 group at one side and one $(HO)PO_3$ tetrahedron at the other side. Identity along the undulated chains is reached after a sequence of six tetrahedra in the central backbone, representing a sechser single chain; see also added explanation to reference 3 (Liebau).[3]

Table 1. Crystallographic data and refinement results of H_2DAP-Mn, H_2PIP-Mn, and H_2DABCO-H_2PIP-Mn.

	H_2DAP-Mn	H_2PIP-Mn	H_2DABCO-H_2PIP-Mn	H_2DABCO-H_2PIP-Mn
M_r	454.62	466.63	478.64	478.64
space group	*Pmc*2$_1$ (no. 26)	*Ima*2 (no. 46)	*Ima*2 (no. 46)	*Ima*2 (no. 46)
a [pm]	1259.43(5)	1257.9(1)	1262.90(7)	1260.56(9)
b [pm]	949.86(5)	948.69(8)	961.05(5)	957.68(7)
c [pm]	1135.92(5)	1158.19(8)	1151.42(7)	1150.4(1)
V [10^6 pm^3]	1358.9(1)	1382.2(2)	1397.49(14)	1388.8(2)
Z	4	4	4	4
ρ_{calcd} [g cm^{-3}]	2.222	2.242	2.275	2.289
μ[a] [mm^{-1}]	1.403	1.383	1.371	0.715
crystal size [mm^3]	0.2×0.05×0.03	0.08×0.03×0.03	0.06×0.06×0.02	0.06×0.06×0.02
crystal habit	colorless, prism	colorless, prism	colorless, plate	colorless, plate
T [K]	295(2)	295(2)	295(2)	120(2)
2θ range[°]	3.24–68.68	5.38–64.38	5.32–67.50	4.22–51.68
measured data	15341	5987	7968	9698
unique data	5249	2249	2535	2825
observed data [$F_o > 4\sigma(F_o)$]	4917	2077	2358	2357
parameters	296	154	148	148
R_{int}/R_σ	0.030/0.037	0.038/0.053	0.028/0.034	0.064/0.059
*R*1 [$F_o > 4\sigma(F_o)$]	0.031	0.035	0.030	0.041
*R*1 (all data)	0.036	0.041	0.033	0.057
*wR*2 [$F_o > 4\sigma(F_o)$]	0.065	0.068	0.073	0.081
*wR*2 (all data)	0.067	0.070	0.076	0.085
goodness-of-fit on F^2	1.038	1.042	1.106	1.005
Flack parameter χ	0.40(1)	0.01(2)	−0.004(16)	−0.01(3)
max/min residual electron density [e×10^{-6} pm^{-3}]	0.49/−0.49	0.75/−0.45	0.49/−0.36	0.53/−0.50

[a] $Ag_{K\alpha}$ for the low-temperature measurement for rest $Mo_{K\alpha}$.

Abstract in German: *Die Templat-gestützten mikroporösen Verbindungen [H_2(Templ.)][Mn^{II}{$B_2P_3O_{12}$(OH)}], [template: 1,3-diaminopropan, $C_3H_{10}N_2$ (DAP); piperazin, $C_4H_{10}N_2$ (PIP); 1,4-diazacyclo[2.2.2]octan, $C_6H_{12}N_2$ (DABCO)] wurden unter milden hydrothermalen Bedingungen hergestellt. Die Kristall-sturkturen (H_2DAP-Mn:* Pmc2$_1$ *(no. 26),* a = *1259.43(5),* b = *949.86(5),* c = *1135.92(5) pm,* Z = *4; H_2PIP-Mn:* Ima2 *(no. 46),* a = *1257.9(1),* b = *948.69(8),* c = *1158.19(8) pm,* Z = *4; H_2DABCO-H_2PIP-Mn:* Ima2 *(no. 46),* a = *1262.90(7),* b = *961.05(5),* c = *1151.42(7) pm,* Z = *4) enthalten identische Gerüstverknüpfungen [Mn^{II}-{$B_2P_3O_{12}$(OH)}]$^{2-}$ mit unterschiedlichen Querschnitten der Strukturkanäle, die eine formselektive Steuerung der Kanalquerschnitte durch die Templatmolekule anzeigt ist. Die Ergebnisse der Synthesen, der chemischen Analysen und der Strukturverfeinerungen werden durch detaillierte ab-initio-Rechungen (Struktur-Optimierungen) gestützt.*

A loop-branched dreier single chain[3] with the same tetrahedral connectivity, but in a linear (straight) arrangement, is known from the crystal structure of $Na_5[B_2P_3O_{13}]$.[4] The conformational variations of this kind of loop-branched borophosphate chains already indicate its significant shape flexibility. The three-dimensional structural framework of H_2DAP-Mn and H_2PIP-Mn is constructed from the loop-branched borophosphate sechser single chains together with distorted $Mn^{II}O_6$ octahedra ($CN(Mn^{II}) = 5$ (207–235 pm) + 1(255–266 pm); see Tables 2 and 3) by sharing common oxygen corners. The crystal structure of H_2PIP-Mn is an isotype of the respective Co^{II} and Zn^{II} compounds (denoted as H_2PIP-Co and H_2PIP-Zn).[5] Experiments made in order to prepare H_2DAP-Co and H_2DAP-Zn failed and no templated borophosphate was formed. In case of DABCO, again no templated Co–borophosphate could be obtained, and in the Zn system only a very complex borophosphate [Zn_3-$(H_2DABCO)_3$][$B_6P_{12}O_{39}(OH)_{12}$]·(H_2DABCO)[HPO_4][6] was isolated. This means that the anionic partial structure [Mn^{II}-

 © 2007 Wiley-VCH Verlag GmbH & Co. KGaA, Weinheim

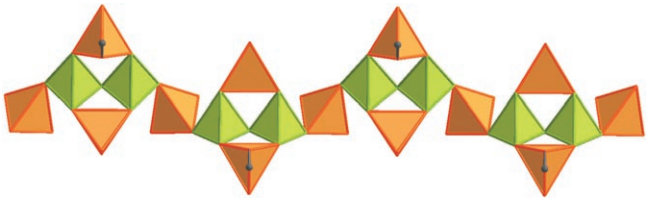

Figure 1. Loop-branched borophosphate single chain running along [100] in the crystal structures of H_2(template)-Mn. BO_4 tetrahedra: green, PO_4 tetrahedra: orange, protons: black spheres.

$\{B_2P_3O_{12}(OH)\}]^{2-}$ is particularly characterized by a pronounced intrinsic flexibility.

As already mentioned, the anionic frameworks $[Mn^{II}\{B_2P_3O_{12}(OH)\}]^{2-}$ of H_2DAP-Mn and H_2PIP-Mn are constructed with identical structural connectivity. The frameworks are characterized by three different channel systems running along [100], [011], and [01$\bar{1}$] directions. Figure 2 shows a projection on the crystal structure of H_2DAP-Mn and H_2PIP-Mn viewed along [100] and showing the different shapes of the templates taking over control of the channel shapes (more elliptical in case of H_2DAP-Mn, and roughly isometric in case of H_2PIP-Mn). The diprotonated organic molecules are fixed within the channels through hydrogen bonds (N–H···O) to oxygen atoms positioned at the inner walls (distances H···O range between 145 and 168 pm). The inner walls of the channels are formed by nine-membered rings of BO_4 (2×), PO_4 (4×) and MnO_6 (3×) polyhedra with two different and alternating cross sections along [100]. The situation is presented in Figure 3 by showing the linking arrangements of polyhedral edges contributing to the inner channel walls. By fixing one oxygen corner of each of the two ring systems formed by H_2DAP-Mn and H_2PIP-Mn at the same position, the relative structural displacements by changing the template cations become evident. This procedure reflects the enormous flexibility of the framework, which is demonstrated by displacement values up to 243 pm.

To analyse the flexibility of the framework in more detail, electronic structure calculations and geometry optimizations were performed. Both, the X-ray refinements (Table 1) and the structure optimizations of H_2DAP-Mn and H_2PIP-Mn (Table 4) exhibit *Pmc*2_1 and *Ima*2 space groups, respectively. Experimental and computed atomic positions and lattice parameters of both compounds were found in very good agreement with the only exception that the positions of the hydrogen atoms were difficult to obtain from the X-ray data.

Apart from elucidating the crystal structure of the templated borophosphates, the calculations also allow the study of energy changes related to modifications of the lattice framework by insertion of different templates. The incorporation energy may be estimated by subtracting the energy related to the isolated template from the total energy of the whole compound. The resulting energy difference ΔE reflects the template–framework interactions and the energy related to structural changes of both the templates and the inorganic framework. The empty framework exhibits a negative net charge and cannot be investigated as a stand-alone system. Absolute incorporation energies are hence not very

Table 2. Selected interatomic distances [pm] and angles [°] in the crystal structure of H_2DAP-Mn.

	Distance [pm]		Angle [°]
Mn1–O17	211.3(2)	O17-Mn1-O1(×2)	93.78(4)
Mn1–O1(×2)	211.38(14)	O1-Mn1-O1	170.67(9)
Mn1–O13	219.0(2)	O17-Mn1-O13	101.79(9)
Mn1–O12	235.8(2)	O1-Mn1-O13(×2)	91.89(5)
Mn1–O7	255.3(2)	O1-Mn1-O12(×2)	86.76(5)
		O1-Mn1-O7(×2)	86.30(4)
		O13-Mn1-O12	159.97(8)
		O17-Mn1-O7	178.28(8)
		O17-Mn1-O12	98.24(9)
		O13-Mn1-O7	76.49(8)
		O12-Mn1-O7	83.48(8)
Mn2–O7	207.3(2)	O18-Mn2-O16	96.39(10)
Mn2–O16	208.8(2)	O18-Mn2-O15(×2)	101.87(9)
Mn2–O15	212.6(2)	O18-Mn2-O8(×2)	95.79(4)
Mn2–O8(×2)	219.56(15)	O16-Mn2-O8(×2)	89.58(4)
Mn2–O3	266.2(2)	O15-Mn2-O8(×2)	88.59(4)
		O8-Mn2-O3(×2)	84.21(4)
		O8-Mn2-O8	168.42(8)
		O18-Mn2-O3	179.66(9)
		O16-Mn2-O3	83.96(8)
		O15-Mn2-O3	77.78(8)
		O16-Mn2-O15	161.74(9)
P1–O17	149.7(2)	O17-P1-O4(×2)	110.61(8)
P1–O13	152.2(2)	O13-P1-O4(×2)	109.23(8)
P1–O4(×2)	157.69(15)	O4-P1-O4	104.31(12)
		O17-P1-O13	112.53(13)
P2–O16	147.6(3)	O16-P2-O14(×2)	112.41(9)
P2–O14(×2)	155.31(15)	O14-P2-O6(×2)	106.28(9)
P2–O6	156.0(3)	O14-P2-O14	107.08(12)
		O16-P2-O6	111.95(14)
P3–O18	148.4(2)	O18-P3-O10(×2)	108.84(9)
P3–O15	150.3(2)	O15-P3-O10(×2)	109.32(8)
P3–O10(×2)	158.62(15)	O10-P3-O10	103.12(12)
		O18-P3-O15	116.55(14)
P4–O8	150.46(15)	O8-P4-O2	110.31(8)
P4–O1	151.02(15)	O8-P4-O9	106.78(9)
P4–O9	156.56(15)	O1-P4-O9	110.18(8)
P4–O2	157.49(16)	O8-P4-O1	115.41(10)
		O1-P4-O2	106.05(8)
		O9-P4-O2	107.92(9)
P5–O12	148.5(2)	O12-P4-O5(×2)	113.59(8)
P5–O5(×2)	155.87(15)	O5-P4-O11(×2)	105.84(9)
P5–O11	156.4(3)	O12-P4-O11	111.95(14)
		O5-P4-O5	105.34(12)
B1–O2	145.6(2)	O2-B1-O3	111.87(17)
B1–O3	146.2(2)	O2-B1-O10	110.63(16)
B1–O10	147.6(3)	O3-B1-O10	109.99(16)
B1–O14	148.9(3)	O2-B1-O14	105.15(15)
		O3-B1-O14	110.77(17)
		O10-B1-O14	108.27(16)
B2–O9	144.4(2)	O9-B2-O7	111.68(16)
B2–O7	147.3(2)	O9-B2-O4	111.94(16)
B2–O4	149.2(3)	O7-B2-O4	108.91(16)
B2–O5	150.0(3)	O9-B2-O5	105.38(15)
		O7-B2-O5	109.81(16)
		O4-B2-O5	109.03(16)
N1–C1	147.4(4)	N1-C1-C3	111.4(2)
N2–C2	148.9(4)	N2-C2-C3	112.6(2)
C1–C3	150.5(4)	C1-C3-C2	106.5(2)
C2–C3	151.4(4)		

 © 2007 Wiley-VCH Verlag GmbH & Co. KGaA, Weinheim

Table 3. Selected interatomic distances [pm] and angles [°] in the crystal structure of H_2PIP-Mn.

	Distance [pm]		Angle [°]
Mn1−O4	207.1(3)	O4-Mn1-O8	98.49(12)
Mn1−O8	212.4(3)	O4-Mn1-O1(×2)	93.74(5)
Mn1−O1(×2)	213.45(19)	O8-Mn1-O1(×2)	91.66(5)
Mn1−O5	229.8(3)	O1-Mn1-O1	171.27(11)
Mn1−O9	255.8(3)	O1-Mn1-O9(×2)	86.11(5)
		O1-Mn1-O5(×2)	87.33(6)
		O4-Mn1-O5	96.85(12)
		O4-Mn1-O9	175.89(11)
		O8-Mn1-O9	85.62(9)
		O8-Mn1-O5	164.65(10)
		O5-Mn1-O9	79.03(9)
P1−O1(×2)	149.94(19)	O1-P1-O1	118.32(17)
P1−O2(×2)	158.18(19)	O1-P1-O2(×2)	105.39(10)
		O1-P1-O2(×2)	109.74(10)
		O2-P1-O2	107.92(14)
P2−O4	148.9(3)	O4-P2-O5	114.10(18)
P2−O5	153.2(3)	O4-P2-O3(×2)	109.82(11)
P2−O3(×2)	156.70(19)	O5-P2-O3(×2)	108.47(10)
		O3-P2-O3	105.82(15)
P3−O8	148.2(3)	O8-P3-O7(×2)	112.19(10)
P3−O7(×2)	155.2(2)	O7-P3-O6(×2)	107.17(11)
P3−O6	156.4(3)	O7-P3-O7	107.29(15)
		O8-P3-O6	110.54(18)
B1−O2	145.6(4)	O2-B1-O9	111.4(2)
B1−O9	146.9(3)	O2-B1-O3	111.2(2)
B1−O3	147.7(3)	O9-B1-O3	109.4(2)
B1−O7	149.0(3)	O2-B1-O7	104.8(2)
		O9-B1-O7	110.6(2)
		O3-B1-O7	109.3(2)
N1−C1	147.1(4)	C1-N1-C2	111.8(3)
N1−C2	148.9(5)	N1-C1-C1	110.8(3)
C1−C1	151.1(8)	N1-C2-C2	111.0(3)
C2−C2	151.6(8)		

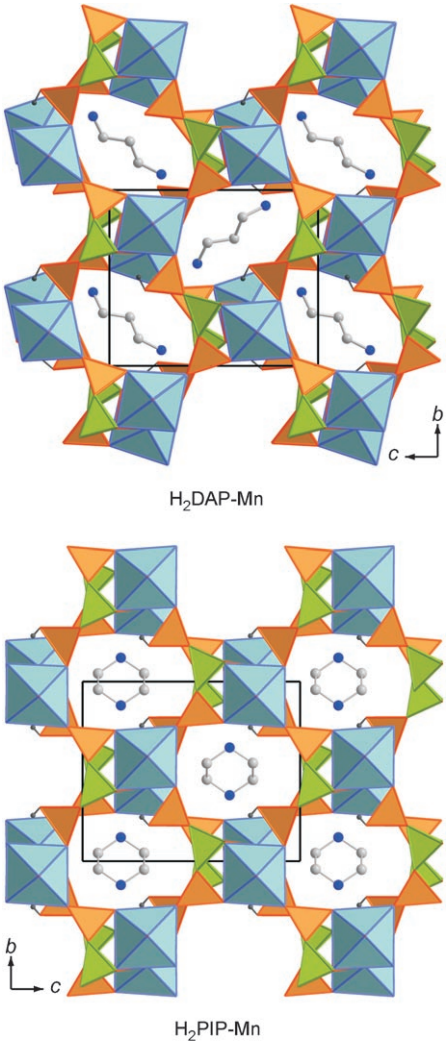

Figure 2. Crystal structures of H_2DAP-Mn ($Pmc2_1$) and H_2PIP-Mn (*Ima*2) viewed along [100], showing the identical framework connectivity, but different channel shapes. MnO_6 octahedra: blue; BO_4 tetrahedra: green; PO_4 tetrahedra: orange; C atoms: light grey spheres; N atoms: blue spheres. Protons omitted for clarity.

meaningful. However, relative differences $\Delta(\Delta E)$ in the incorporation energies related to inserting different template species into the framework can be compared. On this basis H_2PIP-Mn was found to be favored by $\approx 21\,kJ\,mol^{-1}$ over H_2DAP-Mn. The different shapes of the template molecules lead to dramatic deformations within the inorganic framework. While the diprotonated piperazine template is embedded in roughly isometric channels, the linear diprotonated diaminopropane template causes considerable deformation of the skeleton and the formation of channels with an elliptical cross section (Figure 4).

To further elucidate the role of framework deformations, we attempted to incorporate the piperazine template in the inorganic framework of H_2DAP-Mn and to insert the diaminopropane template into the skeleton of H_2PIP-Mn. For this purpose, we exchanged the templates of the relaxed structures (as illustrated in Figure 4) and investigated the structural relaxation from energy minimization runs. For both compounds the inorganic framework was observed to re-adjust to the corresponding template, resulting in almost identical configurations as shown in Figure 2. This numerical experiment underlines the high flexibility of the inorganic framework, which allows large deformations in order to adapt to the geometry of the incorporated template.

Having such a flexible inorganic framework it appeared reasonable to assume that a variety of further template species may be incorporated. Along this line we tried to use diprotonated DABCO as templating agent, which resulted in a hypothetical crystal structure "H_2DABCO-Mn" from the energy-minimization calculations. The result is shown in Figure 4 (right); orthorhombic, *Ima*2, $a = 1302.61$, $b = 993.40$, $c = 1161.87$ pm, $Z = 4$ (see also Table 4). For estimating the stability of this compound we compared the template incorporation energy with the already confirmed compounds H_2DAP-Mn and H_2PIP-Mn. From this "H_2DABCO-Mn" is found to be disfavored over H_2PIP-Mn by $\approx 115\,kJ\,mol^{-1}$,

 © 2007 Wiley-VCH Verlag GmbH & Co. KGaA, Weinheim

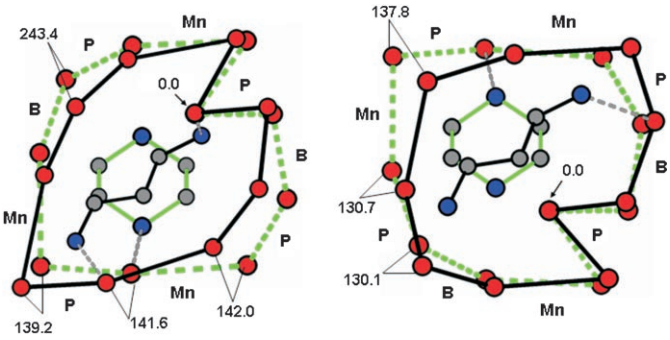

Figure 3. Linking-arrangements of edges (bonding to Mn-, P-, and B-centered polyhedra) contributing to the inner channel walls along [100], of H_2DAP-Mn and H_2PIP-Mn: by fixing one oxygen corner of each of the two ring systems formed by H_2DAP-Mn and H_2PIP-Mn, respectively, at the same position, the relative structural displacements by changing the template cations become evident. Maximum displacement values up to 243 pm. O atoms: red sphere, N atoms: blue spheres, C atoms: grey spheres. Green lines: H_2PIP-Mn; Black lines: H_2DAP-Mn.

Table 4. Crystallographic data from ab initio structure calculations of H_2DAP-Mn, H_2PIP-Mn, and "H_2DABCO-Mn".

	H_2DAP-Mn	H_2PIP-Mn	"H_2DABCO-Mn"
M_r	454.62	466.63	492.67
space group	$Pmc2_1$ (no. 26)	*Ima*2 (no. 46)	*Ima*2 (no. 46)
a [pm]	1287.56	1278.06	1302.61
b [pm]	981.26	960.35	993.40
c [pm]	1141.96	1183.87	1161.87
V [10^6 pm^3]	1442.78	1453.81	1503.47
Z	4	4	4

but it seemed to be not totally impossible to really prepare the compound even with this high energy difference. Therefore, experiments were performed to synthesize "H_2DABCO-Mn". However, the purely templated compound was not obtained. Instead, it was found that during the templating reaction DABCO was partially decomposed to PIP, and the templated crystalline Mn–borophosphate is clearly described with the chemical formula H_2DABCO-H_2PIP-Mn (Table 5), representing a 1:1 molar ratio of disordered templates incorporated (based on corresponding results from X-ray structure determinations, chemical analyses, and TG/DTA investigations; see Experimental Section). Even detailed investigations in low-temperature X-ray data sets (see Table 1) did not give any indication for ordering of the templates (formation of a superstructure). Crystal structure optimization calculations on different ordered models were carried out. All six possible arrangements of two H_2PIP and two H_2DABCO templates in the four cross-section "channels" were relaxed without symmetry constraints (i.e. calculations in space group *P*1). Details of the resulting cell parameters of six models (**1**–**6**) are given in Table 6. The total energy differences of the different arrangements are below 6 kJ mol^{-1}. The relaxed structures were then checked for additional symmetry.[15,16] In fact, H_2DABCO-H_2PIP-Mn was found to be disfavored over H_2PIP-Mn by only $\approx$61 kJ mol^{-1}, which is significantly lower than $\approx$115 kJ mol^{-1} for the hypothetical "H_2DABCO-Mn".

The crystal structure of H_2DABCO-H_2PIP-Mn is shown in Figure 5 (viewed along [100]; space group *Ima*2). As for H_2PIP-Mn (also space group *Ima*2) the cross section of the channels running along [100] is nearly isometric. Differences in the cell parameters in going from H_2PIP-Mn to H_2DABCO-H_2PIP-Mn are moderate: *a* (increase of 0.4 % $\approx$5 pm), *b* (increase of 1.3 % $\approx$12.4 pm), *c* (decrease of 0.6 % $\approx$6.8 pm).

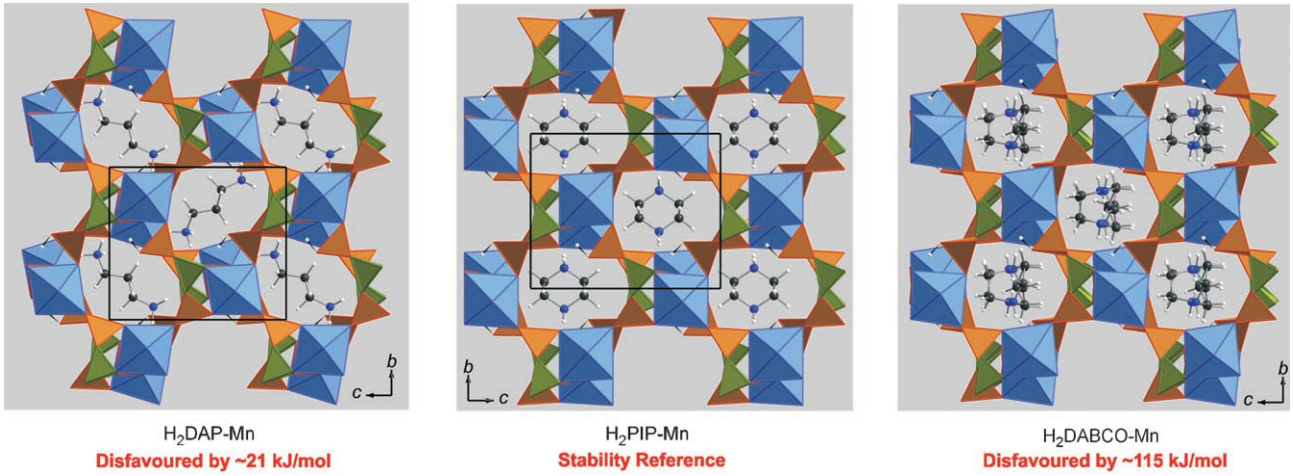

Figure 4. Results of the crystal structure optimizations of H_2DAP-Mn, H_2PIP-Mn, and "H_2DABCO-Mn" viewed along [100]. See also Figure 2. MnO_6 octahedra: blue; BO_4 tetrahedra: green; PO_4 tetrahedra: orange; C atoms: dark grey spheres; N atoms: blue spheres; protons: white spheres. For further details see text.

 © 2007 Wiley-VCH Verlag GmbH & Co. KGaA, Weinheim

Table 5. Selected interatomic distances [pm] and angles [°] in the crystal structure of H_2DABCO-H_2PIP-Mn.

	Distance [pm]		Angle [°]
Mn1−O4	207.7(3)	O4-Mn1-O8	98.22(10)
Mn1−O1(×2)	215.07(15)	O4-Mn1-O1(×2)	94.29(4)
Mn1−O8	218.6(2)	O1-Mn1-O8(×2)	91.40(5)
Mn1−O5	226.1(2)	O1-Mn1-O1	170.49(9)
Mn1−O9	254.53(19)	O1-Mn1-O9(×2)	85.54(4)
		O1-Mn1-O5(×2)	87.47(5)
		O4-Mn1-O5	96.81(10)
		O4-Mn1-O9	174.87(9)
		O8-Mn1-O9	86.90(7)
		O5-Mn1-O9	78.06(7)
		O8-Mn1-O5	164.96(9)
P1−O1(×2)	149.81(15)	O1-P1-O2(×2)	106.20(8)
P1−O2(×2)	157.21(16)	O1-P1-O2(×2)	109.49(8)
		O1-P1-O1	118.01(14)
		O2-P1-O2	106.99(12)
P2−O4	148.6(2)	O4-P2-O3(×2)	109.44(9)
P2−O5	152.2(2)	O5-P2-O3(×2)	109.10(8)
P2−O3(×2)	157.33(16)	O3-P2-O3	104.20(12)
		O4-P2-O5	115.00(14)
P3−O8	147.9(2)	O8-P3-O7(×2)	113.09(9)
P3−O7(×2)	153.80(17)	O7-P3-O6(×2)	106.97(9)
P3−O6	155.5(3)	O7-P3-O7	106.01(12)
		O8-P3-O6	110.31(15)
B1−O2	144.5(3)	O2-B1-O3	111.80(16)
B1−O3	147.0(3)	O2-B1-O9	112.07(17)
B1−O9	147.9(2)	O3-B1-O9	109.13(17)
B1−O7	149.7(3)	O2-B1-O7	104.71(16)
		O3-B1-O7	109.73(18)
		O9-B1-O7	109.30(16)
N1−C2	138.7(6)	C2-N1-C1	123.4(3)
N1−C1	144.6(4)	C1-N1-C3	117.8(4)
N1−C3	151.7(7)	C1-N1-C4	97.7(3)
N1−C4	162.0(7)	C3-N1-C4	99.6(4)
C1−C1	148.1(6)	N1-C1-C1	114.28(18)
C2−C2	153.8(12)	N1-C2-C2	109.6(4)
C3−C4	158.0(10)	N1-C3-C4	111.3(5)
		C3-C4-N1	106.9(5)

Table 6. Crystallographic data from ab initio structure calculations of six ordered models of H_2DABCO-H_2PIP-Mn (**1**–**6**).

Model	**1**	**2**	**3**	**4**	**5**	**6**
M_r	478.64	478.64	478.64	478.64	478.64	478.64
space group	*Pma*2	*Pma*2	*Pma*2	*Pma*2	*Ima*2	*Ima*2
a [pm]	1291.16	1291.12	1292.93	1292.68	1290.08	1289.71
b [pm]	977.48	977.48	971.49	971.46	971.86	971.70
c [pm]	1172.95	1173.11	1180.10	1179.84	1183.07	1182.72
V [10^6 pm^3]	1480.36	1480.53	1482.36	1481.63	1483.31	1482.20
Z	4	4	4	4	4	4

Conclusion

We presented the preparation and characterization of templated compounds $[H_2(Templ.)][Mn^{II}\{B_2P_3O_{12}(OH)\}]$ that revealed microporous inorganic framework structures which contain an identical framework connectivity and channel-systems with high structural flexibility. The shape of the channels is controlled by the shape of the template species incorporated. The maximum of possible structural deformations in going from the isometric cross-sectional shape of the channels to more elliptic shapes is not clearly defined (reached) at present. As a further perspective we think about a scenario in which the ability of significant "breathing" of an inorganic framework may support and control the direction of a chemical reaction running inside microchannels.

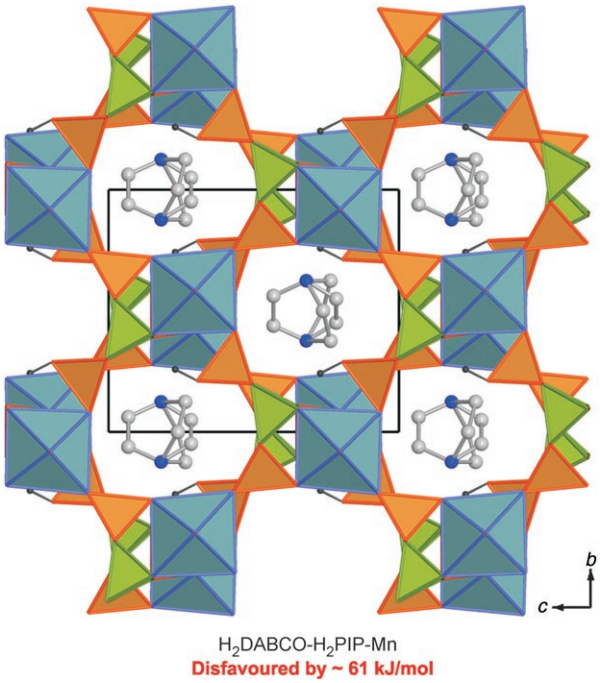

Figure 5. Crystal structure of H_2DABCO-H_2PIP-Mn viewed along [100] showing disordered templates (1:1 molar ratio) inside the channels. The stability of this compound is disfavored $\approx$61 kJ mol^{-1} over that of H_2PIP-Mn (see Figure 4). MnO_6 octahedra: blue; BO_4 tetrahedra: green; PO_4 tetrahedra: orange; C atoms: grey spheres; N atoms: blue spheres. Protons omitted for clarity. For further details see text.

Experimental Section

Preparation and analytical characterization: H_2DAP-Mn and H_2PIP-Mn were synthesized under mild hydrothermal conditions. The starting mixtures (see below) were heated to about 333 K in deionized water (7.5 mL) and treated under stirring for 2 h. Meanwhile 37% HCl (0.75 mL) was added to adjust the pH value to 1.5. The clear pale-pink solution was filled into Teflon autoclaves (V=20 mL, filling degree 30%), and held at 443 K for one week under autogenous pressure. The reaction products were separated by filtering, washed with deionized water and dried at 333 K in air. 1) H_2DAP-Mn: $MnCl_2$ (0.3775 g), H_3BO_3 (0.3710 g), 1,3-diaminopropane ($C_3H_{10}N_2$, DAP) (0.822 g), and 85% H_3PO_4 (1.2682 g) (molar ratio=3:6:11:11). 2) H_2PIP-Mn: $MnCl_2$ (0.3775 g), H_3BO_3 (0.3710 g), piperazine ($C_4H_{10}N_2$, PIP) (0.2585 g) and 85% H_3PO_4 (1.2682 g) (molar ratio=3:6:3:11). The same compound is formed by using the molar ratio as used for synthesis of H_2DAP-Mn.

 © 2007 Wiley-VCH Verlag GmbH & Co. KGaA, Weinheim

H_2DABCO-H_2PIP-Mn was prepared under same conditions as H_2DAP-Mn and H_2PIP-Mn, except for the molar ratio of the components and the reaction time. $MnCl_2$ (0.3775 g), H_3BO_3 (1.4840 g), 1,4-diazacyclo-[2.2.2]octane ($C_6H_{12}N_2$, DABCO) (1.3540 g) and 85 % H_3PO_4 (1.2682 g) (molar ratio = 3:12:12:11) were used. The systematic study of the reaction times showed that the heating time should exceed the period of 10 days. The samples heated for only 7 days contained impurities of the manganese phosphate $Mn_7[PO_3(OH)]_4(PO_4)_2$.[7] The base purity of reported compounds was controlled by using X-ray powder diffraction (Huber Image Foil Guinier Camera G670, $Cu_{K\alpha 1}$ radiation, Ge monochromator).

The chemical compositions of the reported compounds were checked by elemental analyses of the bulk material. Manganese, boron and phosphorus contents were analysed using ICP-OES (VARIAN Vista, radial observation), while a hot extraction method was applied for carbon, nitrogen and hydrogen (LECO CHNS-932). The analytical results are given as follows:

H_2DAP-Mn: elemental analysis calcd (%) for H_2DAP-Mn: Mn 12.08, B 4.76, P 20.44, C 7.93, N 6.16, H 2.88; found: Mn 11.99(5), B 5.33(2), P 22.43(5), C 7.90(4), N 6.09(3), H 2.88(2).

H_2PIP-Mn: elemental analysis calcd (%) for H_2PIP-Mn: Mn 11.77, B 4.32, P 19.91, C 10.30, N 6.00, H 2.81; found: Mn 11.98(8), B 4.54(3), P 20.1(1), C 10.27(5), N 6.13(4), H 2.81(2).

H_2DABCO-H_2PIP-Mn: elemental analysis calcd (%) for H_2DABCO-H_2PIP-Mn: Mn 11.45, B 4.51, P 19.37, C 12.52, N 5.84, H 2.94; found: Mn 11.61(6), B 4.45(1), P 19.45(6), C 12.58(1), N 5.68(4), H 3.01(2).

Thermal analyses of the compounds under consideration were carried out under static air with heating and cooling rates of 5 K min^{-1} up to 1273 K. The TG curves of the three reported compounds show three-step decomposition processes. The weight losses are given as follows: H_2DAP-Mn, 21.59 % (21.25 % calcd, according to a hypothetical weight loss of one $C_3H_{10}N_2$ and 1.5 H_2O per formula unit); H_2PIP-Mn, 24.19 % (24.25 % calcd, according to a hypothetical weight loss of one $C_4H_{10}N_2$ and 1.5 H_2O per formula unit); H_2DABCO-H_2PIP-Mn, 25.82 % (26.30 % calcd, attributing to loss of 0.5 $C_4H_{10}N_2$, 0.5 $C_6H_{12}N_2$ and 1.5 H_2O per formula unit).

Crystal structure determinations: Suitable single crystals of the reported compounds were investigated on a Rigaku AFC7 four-circle diffractometer, equipped with a MERCURY-CCD detector ($Mo_{K\alpha}$ radiation, graphite monochromator, scan types φ and ω) at 295 K and a Stoe IPDS diffractometer ($Ag_{K\alpha}$ radiation, graphite monochromator, scan mode $\Delta\phi = 0.8°$) for the low-temperature measurement (at 120 K), respectively. The collected X-ray data were corrected for Lorentz and polarisation effects. A multiscan absorption correction was applied. The structures were solved by direct methods and refined by full-matrix least-squares methods by using the SHELXS[8] and SHELXL[9] programs included in the WinGX package (Farrugia, L. J., Department. of Chemistry, University of Glasgow, Glasgow, Scotland). After anisotropic refinement of the heavier atoms, all hydrogen atoms were located from the difference Fourier maps and refined without applying any restraints. The crystallographic data and refinement result of H_2DAP-Mn, H_2PIP-Mn and H_2DABCO-H_2PIP-Mn (RT and 120 K) are summarized in Table 1. Atomic coordinates and equivalent displacement parameters of H_2DAP-Mn, H_2PIP-Mn and H_2DABCO-H_2PIP-Mn are given in Table 7–9, respectively. Selected interatomic distances and angles of H_2DAP-Mn, H_2PIP-Mn and H_2DABCO-H_2PIP-Mn are given in Tables 1–3, respectively. CCDC-618722 (H_2DAP-Mn), CCDC-618723 (H_2PIP-Mn), CCDC-618720 (H_2DABCO-H_2PIP-Mn), and CCDC-618721 (H_2DABCO-H_2PIP-Mn at 120 K) contain the supplementary crystallographic data for this paper. These data can be obtained free of charge from The

Table 7. Atomic coordinates and equivalent displacement parameters ($\times 10^4$ pm^2) in the crystal structure of H_2DAP-Mn.

Atom	Site	x	y	z	U_{eq}/U_{iso}[a]
Mn1	2*b*	0.5000	0.37292(5)	0.31809(4)	0.01168(8)
Mn2	2*a*	0.0000	0.17919(5)	0.27506(4)	0.01055(8)
P1	2*b*	0.5000	0.35687(8)	0.60698(6)	0.01032(13)
P2	2*a*	0.0000	0.52412(8)	0.19687(7)	0.01195(13)
P3	2*a*	0.0000	0.06878(8)	0.54304(6)	0.01074(13)
P4	4*c*	0.25167(4)	0.25952(5)	0.37404(5)	0.00917(8)
P5	2*b*	0.5000	0.05751(8)	0.14600(7)	0.01218(13)
B1	4*c*	0.09608(16)	0.3165(2)	0.53293(19)	0.0098(3)
B2	4*c*	0.40272(16)	0.1380(2)	0.51371(19)	0.0100(3)
O1	4*c*	0.33272(11)	0.35486(16)	0.31707(15)	0.0143(3)
O2	4*c*	0.19180(11)	0.35254(15)	0.46768(14)	0.0122(2)
O3	2*a*	0.0000	0.3441(2)	0.46455(19)	0.0101(3)
O4	4*c*	0.40113(11)	0.25525(16)	0.60107(13)	0.0128(3)
O5	4*c*	0.40159(11)	0.99976(17)	0.07824(14)	0.0132(3)
O6	2*a*	0.0000	0.5690(3)	0.3290(2)	0.0205(4)
H1	2*a*	0.0000	0.496(5)	0.359(8)	0.13(4)
O7	2*b*	0.5000	0.1490(2)	0.44237(17)	0.0093(4)
O8	4*c*	0.17344(12)	0.19228(17)	0.29121(12)	0.0142(3)
O9	4*c*	0.30860(12)	0.13694(16)	0.44115(13)	0.0121(3)
O10	4*c*	0.09865(11)	0.16749(16)	0.56992(14)	0.0133(3)
O11	2*b*	0.5000	0.9808(3)	0.2678(2)	0.0246(5)
H2	2*b*	0.5000	1.048(9)	0.334(8)	0.11(3)
O12	2*b*	0.5000	0.2130(2)	0.1593(2)	0.0175(4)
O13	2*b*	0.5000	0.4520(2)	0.4992(2)	0.0151(4)
O14	4*c*	0.09918(11)	0.59401(18)	0.14043(14)	0.0167(3)
O15	2*a*	0.0000	0.0302(2)	0.4148(2)	0.0161(4)
O16	2*a*	0.0000	0.3696(3)	0.1831(2)	0.0205(5)
O17	2*b*	0.5000	0.5619(2)	0.2199(2)	0.0172(4)
O18	2*a*	0.0000	0.0497(3)	0.1282(2)	0.0216(5)
N1	4*c*	0.30207(19)	0.4188(3)	0.0782(2)	0.0216(4)
N2	4*c*	0.23707(19)	0.0889(3)	0.7506(2)	0.0242(4)
C1	4*c*	0.2407(2)	0.3003(3)	0.0294(2)	0.0270(5)
C2	4*c*	0.1974(2)	0.8449(3)	0.3610(3)	0.0287(5)
C3	4*c*	0.2664(3)	0.7237(3)	0.4016(2)	0.0308(6)
H3	4*c*	0.274(3)	0.497(6)	0.058(4)	0.063(13)
H4	4*c*	0.296(3)	0.419(4)	0.150(3)	0.032(9)
H5	4*c*	0.358(3)	0.417(4)	0.058(3)	0.038(11)
H6	4*c*	0.225(2)	0.001(4)	0.749(3)	0.031(9)
H7	4*c*	0.196(3)	0.127(5)	0.690(4)	0.066(14)
H8	4*c*	0.305(4)	0.100(5)	0.757(4)	0.063(14)
H9	4*c*	0.262(3)	0.218(5)	0.068(4)	0.054(13)
H10	4*c*	0.170(3)	0.307(4)	0.045(3)	0.045(10)
H11	4*c*	0.236(5)	0.913(7)	0.426(5)	0.12(2)
H12	4*c*	0.123(3)	0.819(4)	0.334(3)	0.036(9)
H13	4*c*	0.258(4)	0.637(6)	0.347(5)	0.10(2)
H14	4*c*	0.342(4)	0.758(6)	0.389(4)	0.079(16)

[a] Hydrogen atoms were refined with isotropic displacement parameters.

 © 2007 Wiley-VCH Verlag GmbH & Co. KGaA, Weinheim

Table 8. Atomic coordinates and equivalent displacement parameters ($\times 10^4$ pm^2) in the crystal structure of H_2PIP-Mn.

Atom	site	*x*	*y*	*z*	U_{eq}/U_{iso}[a]
Mn1	4*b*	0.7500	0.91166(5)	0.81167(4)	0.00923(12)
P1	4*a*	0.5000	0.0000	0.73191(8)	0.00854(18)
P2	4*b*	0.7500	0.65204(9)	0.03207(8)	0.00953(19)
P3	4*b*	0.7500	0.24022(10)	0.93057(9)	0.01118(19)
B1	8*c*	0.8467(2)	0.4130(3)	0.0826(3)	0.0098(5)
O1	8*c*	0.58081(15)	0.91673(19)	0.79828(17)	0.0134(4)
O2	8*c*	0.94188(15)	0.38937(19)	0.15156(15)	0.0110(4)
O3	8*c*	0.84937(15)	0.55267(19)	0.02646(17)	0.0116(4)
O4	4*b*	0.7500	0.7490(3)	0.9310(3)	0.0183(6)
O5	4*b*	0.7500	0.7728(3)	0.6491(2)	0.0144(6)
O6	4*b*	0.7500	0.3003(3)	0.8048(3)	0.0198(6)
O7	8*c*	0.84939(16)	0.3009(2)	0.99252(17)	0.0154(4)
O8	4*b*	0.7500	0.0840(3)	0.9287(3)	0.0152(6)
O9	4*b*	0.7500	0.4009(3)	0.1530(2)	0.0077(5)
N1	8*c*	0.9455(2)	0.8671(3)	0.1760(3)	0.0196(5)
C1	8*c*	0.9505(3)	0.9549(4)	0.0715(3)	0.0286(8)
C2	8*c*	0.9510(3)	0.9536(4)	0.2832(3)	0.0318(8)
H1	4*b*	0.7500	0.255(9)	0.772(7)	0.09(3)
H2	8*c*	0.876(4)	0.828(4)	0.183(4)	0.049(13)
H3	8*c*	1.000(3)	0.804(3)	0.171(3)	0.012(8)
H4	8*c*	0.947(4)	0.899(4)	0.020(4)	0.047(13)
H5	8*c*	0.883(4)	1.014(5)	0.068(4)	0.048(14)
H6	8*c*	0.881(3)	1.005(4)	0.285(3)	0.030(10)
H7	8*c*	0.948(3)	0.891(4)	0.352(3)	0.025(10)

[a] Hydrogen atoms were refined with isotropic displacement parameters.

Table 9. Atomic coordinates and equivalent displacement parameters ($\times 10^4$ pm^2) in the crystal structure of H_2DABCO-H_2PIP-Mn.

Atom	site	*x*	*y*	*z*	U_{eq}/U_{iso}[a]
Mn1	4*b*	0.2500	0.08952(4)	0.18821(3)	0.01237(9)
P1	4*a*	0.5000	0.0000	0.26936(6)	0.01343(14)
P2	4*b*	0.2500	0.34976(7)	0.96959(6)	0.01520(15)
P3	4*b*	0.2500	0.76418(8)	0.06601(7)	0.01866(16)
B1	8*c*	0.8467(2)	0.4130(3)	0.0826(3)	0.0098(5)
O1	8*c*	0.41971(12)	0.08200(16)	0.20236(15)	0.0200(3)
O2	8*c*	0.05822(12)	0.60694(16)	0.85058(13)	0.0178(3)
O3	8*c*	0.15170(12)	0.44981(16)	0.97799(14)	0.0181(3)
O4	4*b*	0.2500	0.2534(2)	0.0705(2)	0.0261(5)
O5	4*b*	0.2500	0.2208(3)	0.35120(19)	0.0234(5)
O6	4*b*	0.2500	0.7110(3)	0.1935(3)	0.0450(8)
O7	8*c*	0.15273(13)	0.70002(18)	0.00607(15)	0.0239(3)
O8	4*b*	0.2500	0.9180(2)	0.0635(2)	0.0235(5)
O9	4*b*	0.2500	0.59498(19)	0.84681(16)	0.0109(4)
N1	8*c*	0.05055(19)	0.1239(3)	0.8188(3)	0.0349(5)
C1	8*c*	0.0354(4)	0.0614(4)	0.9318(3)	0.0542(11)
C2[b]	8*c*	0.0481(6)	0.0490(6)	0.7159(4)	0.0348(13)
C3[b]	8*c*	0.0426(7)	−0.1241(6)	0.7356(6)	0.0502(19)
C4[b]	8*c*	0.1206(6)	0.0006(6)	0.7614(6)	0.0477(16)
H1	4*b*	0.2500	0.758(6)	0.270(6)	0.072(19)

[a] Hydrogen atoms were refined with isotropic displacement parameters. [b] Occupancy of these atoms is 0.5.

Cambridge Crystallographic Data Centre via www.ccdc.cam.ac.uk/data_request/cif.

Ab initio calculations: Electronic structure calculations and geometry optimizations were performed by using the siesta DFT-package[10,11] applying the GGA functional with the exchange-correlation of Perdew, Burke, Ernzerhof (PBE).[12] The pseudopotentials for the core electrons were created within the Troullier–Martins scheme.[13,14] The generated pseudopotentials of Mn, B, P and O were verified on the basis of test calculations of the crystal structures of MnO[15] and BPO_4.[16] The suitability of the pseudopotentials for C, N, H was confirmed from geometry optimisation of the diaminopropane molecule in vacuum. The $4s^0 3d^5$ electronic state of Mn^{2+} implies spin polarization, which was considered in all calculations for the related compounds. The same reference systems were used for the rectification of the double-zeta polarization (DZP) split valence basis functions and the corresponding soft confinement potentials by means of the downhill simplex method,[17] as described by Artacho et al.[18,19] A cutoff of 200 Ry and a set of 18 k-points ensured total energy convergence.

As far as available, the structures obtained from the X-ray single-crystal refinements were taken as starting models for the theoretical investigations. The configurations were then optimized with respect to lowest energy. Therein the relaxation of the atomic positions was first studied at fixed lattice parameters followed by full-cell refinement in a subsequent simulation run. The geometry optimizations were performed without symmetry constraints on the atomic positions. For better computational performance only the angles of the orthorhombic unit cells were fixed to 90°. After full relaxation the resulting crystal structures were checked for additional symmetry (besides *P*1 of the simulation models) by using the PLATON 2005 package.[20] The crystal structure data resulting from the optimization calculations are given in Tables 4 and Table 6.

Acknowledgements

This work was supported by the Fonds der Chemischen Industrie. The authors would like to thank Anja Völzke for chemical analyses and Susann Müller for thermal analyses.

[1] F. Schüth, *Angew. Chem.* **2003**, *115*, 3730–3750; *Angew. Chem. Int. Ed.* **2003**, *42*, 3604–3622.

[2] a) D. R. Corbin, L. Abrams, G. A. Jones, M. M. Eddy, W. T. A. Harrison, G. D. Stucky, D. E. Cox, *J. Am. Chem. Soc.* **1990**, *112*, 4821–4830; b) G. M. Johnson, B. A. Reisner, A. Tripathi, D. R. Corbin, B. H. Toby, J. B. Parise, *Chem. Mater.* **1999**, *11*, 2780–2787.

 © 2007 Wiley-VCH Verlag GmbH & Co. KGaA, Weinheim

[3] The term "sechser" was coined by Liebau and is derived from the German word sechs, which means six. Similar terms exist for chains comprising three, four, and five tetrahedral centers, namely "dreier", "vierer", and "fünfer" chains, respectively; F. Liebau, *Structural Chemistry of Silicates*, Springer, Berlin, **1985**.
[4] C. Hauf, F. Friedrich, R. Kniep, *Z. Kristallogr.* **1995**, *210*, 446.
[5] G. Schäfer, H. Borrmann, R. Kniep, *Z. Anorg. Allg. Chem.* **2001**, *627*, 61–67.
[6] G. Schäfer, W. Carrillo-Cabrera, S. Leoni, H. Borrmann, R. Kniep, *Z. Anorg. Allg. Chem.* **2002**, *628*, 67–76.
[7] A. Riou, Y. Cudennec, Y. Gerault, *Acta Crystallogr. Sect. C* **1987**, *43*, 821–823.
[8] G. M. Sheldrick, SHELXS-97, Program for Crystal Structure Solution, University of Göttingen, Göttingen (Germany), **1997**.
[9] G. M. Sheldrick, SHELXL-97, Program for Crystal Structure Refinement, University of Göttingen, Göttingen (Germany), **1997**.
[10] P. Ordejon, E. Artacho, J. M Soler, *Phys. Rev. B* **1996**, *53*, R10441–R10444.
[11] J. M. Soler, E. Artacho, J. D. Gale, A. Garcia, J. Junquera, P. Ordejon, D. Sanchez-Portal, *J. Phys. Condens. Matter* **2002**, *14*, 2745–2779.
[12] J. P. Perdew, K. Burke, M. Ernzerhof, *Phys. Rev. Lett.* **1996**, *77*, 3865–3868.
[13] N. Troullier, J. L. Martins, *Phys. Rev. B* **1991**, *43*, 1993–2006.
[14] N. Troullier, J. L. Martins, *Phys. Rev. B* **1991**, *43*, 8861–8869.
[15] S. Sasaki, K. Fujino, J. Takeuchi, R. Sadanaga, *Acta Crystallogr. Sect. A* **1980**, *36*, 904–915.
[16] M. Schmidt, B. Ewald, Yu. Prots, R. Cardoso-Gil, M. Armbrüster, I. Loa, L. Zhang, Y.-X. Huang, U. Schwarz, R. Kniep, *Z. Anorg. Allg. Chem.* **2004**, *630*, 655–662.
[17] W. H. Press, B. P. Flannery, S. A. Teukolsky, W. T. Vetterling, *Numerical Recipes: The Art of Scientific Computing*, Cambridge University Press, Cambridge (UK) **1986**.
[18] J. Junquera, O. Paz, D. Sanches-Portal, E. Artacho, *Phys. Rev. B* **2001**, *64*, 235111.
[19] G. Poulet, P. Sautet, E. Artacho, *Phys. Rev. B* **2003**, *68*, 075118.
[20] A. L. Spek, PLATON, Sectie Kristalen Structuurchemie, University of Utrecht (Netherlands), **2005**.

Received: September 19, 2006
Published online: December 7, 2006

 © 2007 Wiley-VCH Verlag GmbH & Co. KGaA, Weinheim